JOURNAL OF GUIDANCE, CONTROL, AND DYNAMICS
Vol. 17, No. 4, July–August 1994

Stationkeeping of Geostationary Satellites with Simultaneous Eccentricity and Longitude Control

Thomas J. Kelly,* Lisa K. White,† and Donald W. Gamble‡
Space Systems/Loral, Palo Alto, California 94303

Because of increasingly stringent deadband requirements (±0.05°) in conjunction with larger solar radiation perturbations caused by higher area-to-mass ratios on current and future satellites, east/west stationkeeping has become significantly more complicated. An algorithm that simultaneously controls the mean eccentricity and longitudinal motion of a geostationary satellite placed at any station longitude is developed. Eccentricity control is achieved based upon an expanded version of the sun pointing perigee method to include the long-period luni-solar effects in the eccentricity vector targeting scheme. Simultaneous control of the longitudinal motion is achieved by apportioning the required ΔV for eccentricity control amongst N maneuvers to maintain longitude within a ±0.05° deadband. Upon completing the Nth maneuver, the satellite begins a period of free drift with starting conditions coinciding with the optimal free-drift cycle initial conditions. Modeling of the sun, Earth, and moon effects on the satellite's motion allows for an arbitrary station longitude (and in particular for longitudes at or near an equilibrium point). A detailed simulation of the spacecraft's operating environment incorporating the maneuver strategy was used to verify the feasibility of the algorithm and to illustrate its robustness in the presence of measurement and execution errors.

Nomenclature

A/M = spacecraft area-to-mass ratio
a_{syn} = two-body geosynchronous semimajor axis (42,164.2 km)
$E_{Cu,\,l}$ = parameters to control rotation of eccentricity vector
$\boldsymbol{e}$ = eccentricity vector
N = number of maneuvers per stationkeeping cycle ($N \geq 3$)
P_D = duration of free-drift that begins following final maneuver time t_N
P_{EW} = duration of control cycle ($t_N + P_D$: 7–28 days)
RA = right ascension of sun
T_{BD} = maximum allowable burn duration in on-orbit mode (e.g., 0.5 s)
T_{syn} = one sidereal day (86,164.09054 s)
V_{syn} = two-body geosynchronous circular velocity (3.075 km/s)
γ = weighting parameter to shape and size control cycle
Δt_i = time between ith and $i+1$ maneuver ($t_{i+1} - t_i$)
ΔV_{ecc} = tangential ΔV required to change eccentricity vector to target conditons
ΔV_i = tangential ΔV corresponding to ith maneuver
$\Delta\lambda$ = apparent spacecraft longitudinal deviation from station longitude
$\Delta\lambda_D$ = difference between target and initial long-period longitude ($\lambda_T - \lambda_0$)
$|\Delta\lambda|_{max}$ = longitudinal deadband (e.g., ±0.05°)
$\eta_{1,2}$ = parameters to control eccentricity vector magnitude
$\ddot{\lambda}_{ls}$ = longitudinal acceleration due to gravitational attraction of sun and moon
λ_s = nominal station longitude at geostationary altitude
$\ddot{\lambda}_{tess}$ = longitudinal acceleration due to Earth's tesseral harmonics
$(\lambda_i, \dot{\lambda}_i)$ = long-period longitude and drift rate immediately following ith maneuver
$(\lambda_T, \dot{\lambda}_T)$ = long-period longitude and drift rate immediately following Nth maneuver
$(\lambda_0\ \dot{\lambda}_0)$ = initial long-period longitude and drift rate
ν_i = true anomaly at time of ith maneuver
Ω = longitude of ascending node
ω = argument of perigee
ϖ = longitude of perigee ($\Omega + \omega$)

Received Jan. 29, 1991; revision received Oct. 18, 1993; accepted for publication Oct. 19, 1993.

*Engineering Specialist, Orbit Dynamics. Currently Assistant Professor, Mechanical and Aerospace Engineering Department, University of Dayton, Dayton, OH 45469-0210. Member AIAA.
†Engineering Specialist, Orbit Dynamics. Member AIAA.
‡Senior Engineering Specialist, Dynamics and Controls. Member AIAA.

I. Introduction

METHODS of orbital control of geostationary satellites is of continuing interest due to stringent constraints imposed upon the satellite motion by ground-based antennas. The two traditional aspects of orbital control are referred to as north/south (N/S, which controls excursions in latitude) and east/west (E/W, which controls excursions in longitude). The subject of this paper is the E/W control of a geostationary satellite in so far as it can be treated independently of N/S control. In particular, when the N/S stationkeeping is performed (approximately nine times per year), there is coupling with the motion in the E/W direction. This contribution is due in part to thruster canting but mainly from the thrusters' plume impingement on the solar array panels. The change in angular momentum resulting from these torques is compensated by the attitude control system whereby a net ΔV is imparted in both the tangential and radial directions. These in-plane components can be calculated while performing the N/S maneuver and can therefore be canceled upon completing the N/S stationkeeping.

For geostationary satellites, the longitudinal behavior is governed by the Earth's tesseral harmonics and the gravitational effects of the sun and moon. In general, the Earth's tesseral harmonics are the dominant contribution, and can be considered constant over longitudinal variations of less than 1 deg.[1-3] For satellites stationed at or near the equilibrium points, the longitudinal acceleration due to the Earth ($\ddot{\lambda}_{tess} \approx 0$) is small in compari-

son with that due to the sun and moon ($\ddot{\lambda}_{ls}$). The approximate longitude of these points are 11.512°W, 74.942°E, 105.088°W, and 161.899°E. Because the luni-solar effects dominate the mean longitudinal behavior near the equilibrium points, an accurate model of the sun and moon's effects must be used to target the longitude and drift rate needed to initiate a proper free-drift cycle. Figure 1 illustrates the long-period behavior of the longitudinal acceleration at geostationary radius corresponding to six different station longitudes for a duration of one month. This figure shows, for example, that the longitudinal motion of a spacecraft at longitude 158°E is strongly influenced by the effects of the moon. Note that in this region the sign of $\ddot{\lambda}_{tess} + \ddot{\lambda}_{ls}$ is time varying with a period of approximately 13.6 days. Away from this equilibrium point, $\ddot{\lambda}_{tess} + \ddot{\lambda}_{ls}$ has the same oscillations in amplitude but is constant in direction and dominated by the effects of the Earth's tesseral harmonics. The daily averaged, long-period longitudinal acceleration averaged over the E/W stationkeeping cycle (e.g., 7–28 days) is of particular interest to the targeting strategy. The dashed curves in Fig. 1 are a running average of the solid curves. Hence, this figure further illustrates the complexity of E/W stationkeeping near an equilibrium point in that the sign on the average longitudinal acceleration is time dependent.

Addressing the more general case of a time-varying long-period longitudinal acceleration by including luni-solar effects allows the E/W stationkeeping algorithm discussed in this paper to be independent of any particular station longitude. Similarly, the target conditions for the start of the free drift will also be considered variable. These generalizations serve to increase the complexity of the E/W stationkeeping algorithm developed herein over previous methods. If the long-period longitudinal acceleration were constant over the duration of the free drift, the satellite's optimal trajectory (as defined by Kamel[4,5] and Wagner[4] and Kamel et al.[5]) in the long-period longitudinal phase plane (λ, $\dot{\lambda}$) would describe a parabola, centered about the station longitude λ_s with its vertex on the longitudinal axis and its drift rate symmetric about this axis. Such a trajectory begins and ends on the same boundary of the longitudinal deadband with its turning point on the opposite boundary. This permits the spacecraft maximum excursion within the allowable deadband, yielding the most time between stationkeeping maneuvers. Since the long-period longitudinal acceleration is not truly constant, this symmetry cannot be achieved.

To reduce the E/W excursions of a satellite, tight control of the eccentricity vector $\boldsymbol{e}$ must also be maintained. The dominant effects on $\boldsymbol{e}$ are due to solar radiation pressure (which is proportional to the satellite area-to-mass ratio A/M)[6] and luni-solar gravitation. The Earth's gravitational effects due to the tesseral harmonics have little contribution to its long periodic behavior.[7] Solar radiation pressure causes $\boldsymbol{e}$ to rotate perpendicular to the Earth-sun line and with the same sense as the orbital velocity. If allowed to proceed naturally, the eccentricity vector would describe an ellipse (in the orbit plane), nearly a circle, of a size that may not be contained by the bounds required for E/W stationkeeping. Superimposing the luni-solar effects onto this motion adds a long-period variation to its rotation rate and in its length.

Targeting eccentricity is complicated by seasonal variations in the effects due to solar radiation pressure. In addition the lunar effects also vary the eccentricity behavior with a fundamental period of approximately 13.6 days. The steady-state eccentricity vector (which describes the solar radiation pressure ellipse) rotates about its inertial center (assuming small eccentricity), completing one cycle every year. However, the sun and moon cause local variations in this rotation rate that must be accounted for in the targeting scheme. As the mean eccentricity vector approaches a cusp, its rate of rotation decreases, completely stops momentarily, and may even track counter to the sun's direction. In between the cusps, $\boldsymbol{e}$ rotates faster than average. Because the natural rotation of the eccentricity vector varies over a month, the targeting strategy for eccentricity will also need to vary from one cycle to the next. Figure 2 illustrates the osculating and long-period behavior of the uncontrolled eccentricity vector for one year.

Techniques have previously been developed to simultaneously control eccentricity and longitude. In particular, the method developed by Eckstein[8] does not explicitly include the luni-solar effects but uses an iterative control scheme requiring operator intervention to optimize "strategy parameters." Eckstein considers only stationkeeping cycles consisting of one, two, or three maneuvers. Gartrell[9] also ignores the luni-solar contribution in his stationkeeping algorithm designed for small

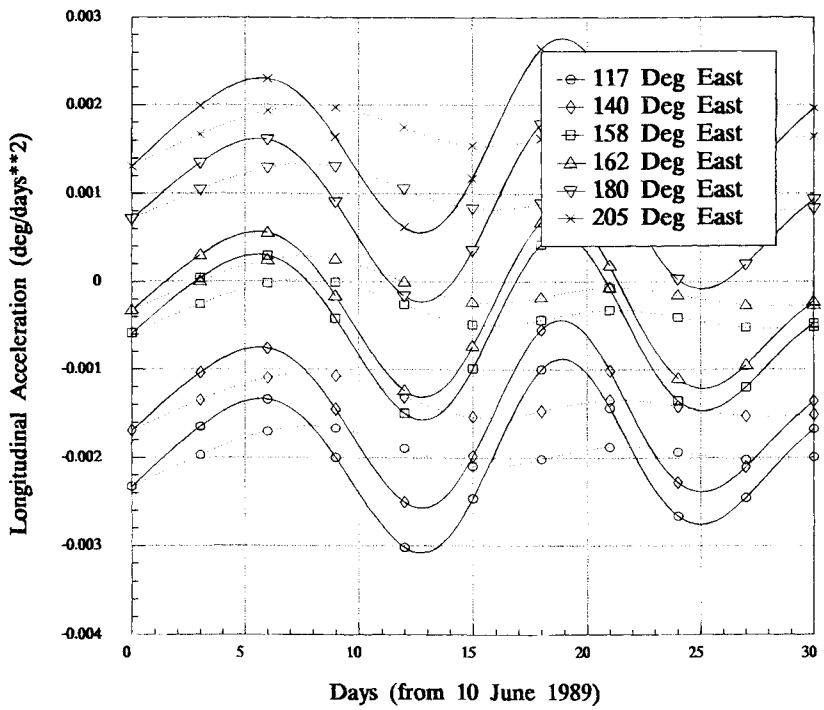

Fig. 1 Long-period longitudinal acceleration ($\ddot{\lambda}_{tess} + \ddot{\lambda}_{ls}$).

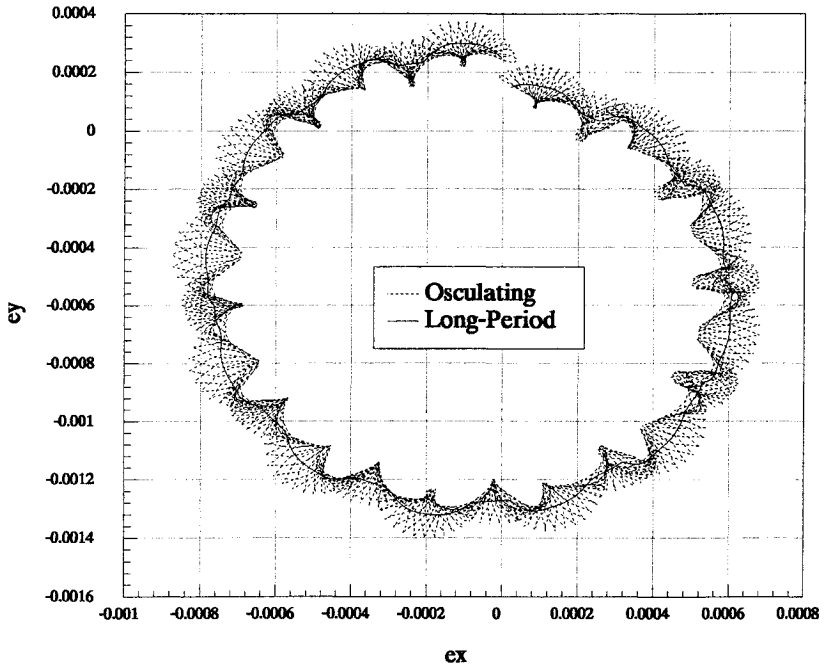

Fig. 2 Uncontrolled eccentricity vector components (one year).

satellites and does not generalize the maneuver strategy to an arbitrary number of maneuvers. Kechichian[10] studied a method for simultaneous eccentricity and longitude control based upon targeting osculating conditions and concluded that the technique would cause longitude to deviate from a specified deadband ($\pm 0.05°$) after only a few cycles (provided the orbit is not updated from cycle to cycle). Many of the ideas previously put forth in the literature are embodied in this work along with several significant technical and operational advancements.

Parameters referred to in this paper in the mean sense correspond to their osculating values minus their associated short-period (i.e., daily) contributions. Short-period terms have periods ranging from 0.25 to 1.2 days and long-period terms from 6.8 days to 18.6 years.[4]

II. Operational Considerations

The ΔV required to perform E/W stationkeeping is relatively small; E/W stationkeeping can be performed by apportioning the total ΔV among N maneuvers (separated nominally by half a sidereal day) where each maneuver satisfies the burn duration constraint. Because of the frequency of the E/W stationkeeping maneuver cycles (e.g., 2–4 times per month), performing small maneuvers significantly reduces their operational complexity.

The size of the total ΔV needed to control the E/W excursions is driven by the location of the longitude and the eccentricity vector relative to the desired target conditions. The longitude must be properly targeted such that the allowable longitudinal deadband is not exceeded during the period of free drift following the Nth maneuver. The magnitude of the eccentricity vector must be held below a constraint value to maintain longitude librations within a prescribed deadband. Keeping eccentricity close to the constraint value helps to reduce propellant usage.[4]

For a given duration of the E/W control cycle P_{EW}, the maximum number of maneuvers permitted is such that the duration of the free-drift period P_D enables the orbital parameters to be updated through the orbit determination process. Additionally, a follow-on period must be available to the operators to plan the next set of maneuvers.

III. Eccentricity Control Strategy

The quantity $\Delta\lambda$ is used to denote the angular difference between the apparent longitude of the satellite λ and the nominal station longitude λ_s. It can be expressed through first order in the eccentricity e as

$$l = GHA + \lambda_s \text{ (local sidereal time of the station)} \quad (1a)$$

$$\Delta\lambda = (\Omega + \omega) + \nu - l$$

$$= \varpi + M - l - 2e \sin(\varpi - l) + \mathcal{O}(e^2) \quad (1b)$$

where GHA is the Greenwich hour-angle, $\varpi = \Omega + \omega$ the longitude of perigee, M the mean anomaly, and ν the true anomaly. Hence, the larger the eccentricity, the more pronounced this longitudinal deviation. The importance of this effect on the satellite's longitude is determined by the allowable deadband in longitude ($|\Delta\lambda|_{max}$). To reduce the E/W excursions of a satellite, tight control on the mean longitude and eccentricity must be maintained.

To reduce eccentricity an obvious strategy is to perform circularizing maneuvers. The frequency with which these maneuvers would be required depends upon the individual mission requirements; however, typically they would be needed approximately once per month. Although this is relatively infrequent, the maneuvers are significantly large.

In the interest of saving propellant, a noncircularizing firing strategy referred to as the sun pointing perigee strategy (SPPS)[4] was developed. This strategy allows a significant reduction in propellant usage, though the maneuvers need to be performed more frequently. The SPPS maintains the eccentricity vector pointing generally in the direction of the sun. The maneuver sequence is initiated with the eccentricity vector leading the Earth-sun line (in general). These maneuvers are performed to set the eccentricity vector to lag the Earth-sun line. The effects of solar radiation pressure will naturally drive the eccentricity vector to lead the Earth-sun line once again, and the process is repeated. In this way the eccentricity vector is made to librate about the Earth-sun line, which is the basic idea behind the SPPS.

For spacecraft with a large A/M, the SPPS (which is based on the geometry of the solar radiation pressure ellipse) was found to be inadequate for purposes of tight longitudinal control (e.g., $\pm$ 0.05°). Therefore, a new eccentricity targeting scheme was developed that in addition controls the magnitude of the eccentricity vector. The new strategy extends the SPPS by

propagating the mean uncontrolled eccentricity vector forward (i.e., without maneuvers) to the end of the next drift cycle. Using this portion of the undisturbed eccentricity profile, one can determine the mean behavior of the eccentricity vector due to the solar radiation pressure and the luni-solar gravitational attraction. Target conditions are obtained by translating this mean eccentricity arc relative to the average Earth-sun line and into the eccentricity constraint circle (Fig. 3). The midpoint of this arc is located on the average Earth-sun line (minus a small bias). Control parameters are introduced to limit the amount that the eccentricity vector is allowed to change in moving from its initial value $\boldsymbol{e}_0$ to the target value $\boldsymbol{e}_T$. Gantous[11] included some of the luni-solar effects in her amendment to the SPPS but did not include the local variations that are inherent to the mean eccentricity arc.

The eccentricity control strategy, used to determine the ΔV required to place the initial eccentricity at the target conditions that will initiate a proper drift cycle, makes use of the following geometric relations. The components of the mean eccentricity vector in the geocentric-equatorial inertial system XYZ and the rotating system xyz are denoted as $\boldsymbol{e} = [e_X e_Y]^T_{XY} = [e_x e_y]^T_{xy}$, where the xyz system rotates about the Z-axis system with the x axis tracking the sun and in advance of the X axis by the right ascension of the sun RA. The inertial angle for the mean eccentricity vector (i.e., the longitude of perigee) is simply $\varpi = \tan^{-1}(e_Y/e_X)$, which is the longitude of the ascending node plus the argument of perigee. The components of the eccentricity vector projected onto and normal to the average Earth-sun line are subscripted by 0 for the initial time t_0 (i.e., start of the control cycle) and denoted as $\boldsymbol{e}_0 = [e_0 \cos(\varpi_0 - RA)\, e_0 \sin(\varpi_0 - RA)]^T_{xy}$. Similarly, these components are subscripted by F for the final time t_F (i.e., end of the free drift) and subscripted by T for the target time t_T (i.e., start of the free drift).

In targeting eccentricity, a more propellant-efficient strategy is one that maintains the eccentricity vector as close to the constraining value E_c as possible. The parameter E_c is the radius of the eccentricity constraint circle and represents the absolute maximum value permitted for the eccentricity. Based on Eq. (1), the following expression is used to determine E_c:

$$E_c = (2|\Delta\lambda|_{\max} - E_{\text{mar}} - \delta\lambda_{sdb})/4 \tag{2}$$

where $|\Delta\lambda|_{\max}$ is the longitudinal deadband (e.g., $\pm 0.05°$), E_{mar} the margin of safety (accounting for systematic errors and unmodeled dynamics), and $\delta\lambda_{sdb}$ the soft longitudinal deadband [accounting for modeled dynamics; see Eq. (18)]. Using the SPPS, E_{mar} accounts for about 30% of the total longitudinal deadband, which results in constraining the eccentricity to about $E_c = 0.00015$.[4] By incorporating the luni-solar effects directly into the eccentricity targeting strategy, this figure has been reduced to 20%, which has enabled eccentricity to be controlled to $E_c = 0.000349$, for a 7-day control cycle, and $E_c = 0.000262$, for a 14-day control cycle. Reducing E_{mar} allows for a more relaxed control of eccentricity and therefore a more efficient use of propellant. In constraining the length of $\boldsymbol{e}$ to E_c, this may require maneuvers to be performed that not only reduce the magnitude of the eccentricity vector but also increase its magnitude.

The amount the eccentricity magnitude is adjusted is determined by the x component of the eccentricity vector and is constrained by the control parameters (η_1, η_2) with $\eta_1 < \eta_2$. Because it is more efficient to locate the maneuvers close to the crossing of the semilatus rectum and simply rotate the eccentricity vector, η_1 and η_2 limit the angle between the location of a maneuver in the orbit and the perpendicular to the average Earth-sun line. That is, η_2 restricts the maximum (past the crossing of the semilatus rectum), whereas η_1 restricts the minimum (before the crossing of the semilatus rectum) of the true anomaly for the maneuvers. These two parameters hold the location of the firings near the crossing of the semilatus rectum and effectively restrict the amount of ΔV that can contribute to changing the eccentricity magnitude. The y component of eccentricity determines the amount it will be rotated to meet its target conditions and is constrained by the control parameters (E_{c_u}, E_{c_l}); E_{c_u} is the maximum value that the eccentricity vector is allowed to rotate relative to the average Earth-sun line, and E_{c_l} is the bias off this line resulting in a target eccentricity that slightly lags the sun. This parameter prevents undertargeting of the eccentricity vector that initiates the free-drift cycle and

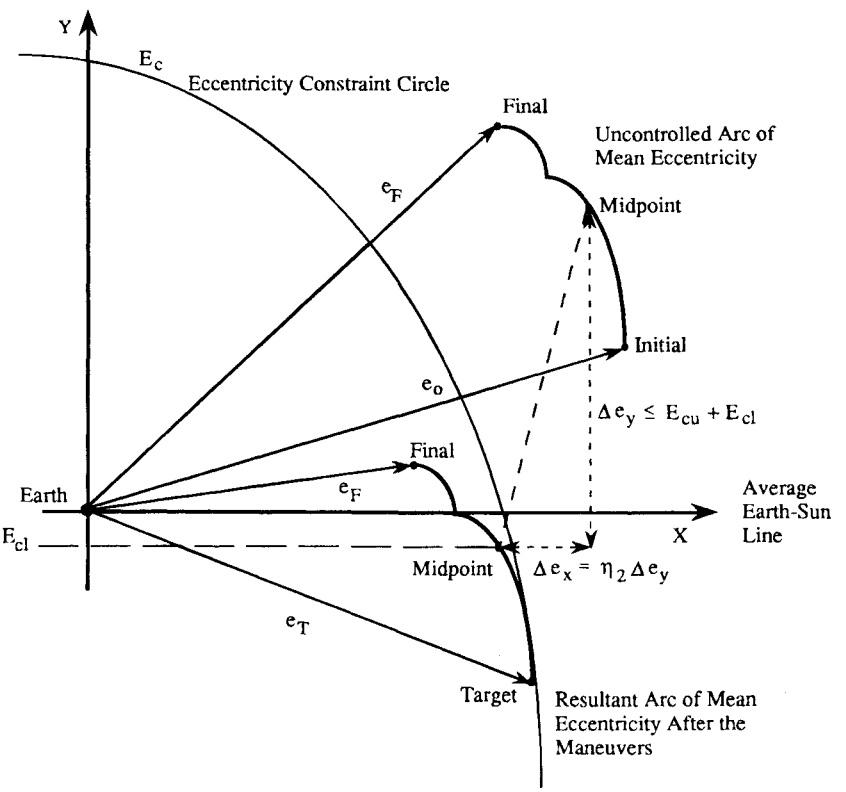

Fig. 3 Eccentricity targeting and control

biases toward slightly overtargeting. This latter set of control parameters is a function of the desired cycle length. Figure 3 illustrates how these parameters limit the changes made to the eccentricity vector. In this illustration, the concavity of the "arc" presented is arbitrary and depends on the relative location of the monthly cycle cusps.

To determine robust values for each of the four eccentricity control parameters, a trend between the individual drift cycles must be characterized during simulated operations. For example, if after several drift cycles the magnitude of the eccentricity vector is increasing/decreasing, then η_1 and η_2 should be decreased/increased. From simulated studies ($\lambda_s = 158°$, $\Delta\lambda_{max} = \pm 0.05°$, $P_{EW} = 7$ or 14 days), this characterization led to the following stable values: $\eta_1 = 0.35$ and $\eta_2 = 0.50$. The trend indicators for E_{c_u} and E_{c_l} are the initial and final resonance angles (α_0, α_F) defined as the included angle between the eccentricity vector and the average Earth-sun line. The initial resonance angle is measured at the start of the free-drift cycle and should be less than zero ($\varpi_0 < RA_0$), and the final resonance angle is measured at the end of the free-drift cycle and should be greater than zero ($\varpi_F > RA_F$). The expected values for the resonance angle will vary depending on the length of the free-drift cycle and the monthly cycle. Ideally they would be equal though opposite in sign; however, the lunar perturbations will prevent this from occurring. If α_F becomes progressively larger and α_0 remains positive (leading the sun) for more than two consecutive scenarios, then the algorithm is undertargeting. To prevent future undertargeting, both E_{c_u} and E_{c_l} should be increased. If the final resonance angle becomes negative and remains negative for more than two consecutive scenarios, then the algorithm is overtargeting, and E_{c_u} and E_{c_l} should be decreased. From simulated studies ($\lambda_s = 158$ or 162°, $\Delta\lambda_{max} = \pm 0.05°$, $P_{EW} = 7$ days), this characterization led to the following stable values: $E_{c_l} = 10^{-5}$ and $E_{c_u} = 4 \times 10^{-5}$. For a 14-day cycle these values could be twice as large. It should be mentioned that the values given for the eccentricity control variables (η_1, η_2, E_{c_l}, E_{c_u}) remained stable even when the solar radiation pressure effects were varied by as much as 20% in the simulated operations.

In the y direction along the uncontrolled mean eccentricity arc, the average change in eccentricity over the free-drift period P_{EW} is

$$\delta e_y = (e_{y0} + e_{yF})/2 \tag{3}$$

By placing a limit on the amount the eccentricity is allowed to rotate to meet its target conditions, the expression for the y direction of the required change becomes

$$\Delta e_y = \min[\max(-E_{c_l}, \delta e_y), E_{c_u}] + E_{c_l} \tag{4}$$

In the x direction along the uncontrolled mean eccentricity arc, the change in eccentricity is taken as the difference between the initial eccentricity vector and the constraining value, whichever is larger:

$$\delta e_x = \max[e_{x_0} - E_c, e_{x_F} - E_c] \tag{5}$$

Constraints are placed on the maximum change allowed in the eccentricity magnitude:

$$\Delta e_x = \max[-\eta_1 \Delta e_y, \min(\eta_2 \Delta e_y, \delta e_x)] \tag{6}$$

Note the allowed change in the x component of the eccentricity vector (measured in the rotating coordinate system) is expressed as a function of the change in the y component of eccentricity. This is to restrict the amount of energy that goes into changing the magnitude of eccentricity as opposed to changing its direction. Magnitude changes to eccentricity are inefficient and, therefore, are scaled by the rotation change. If a large rotational change is required, then the change in eccentricity magnitude is permitted to be larger. Given the components for the change required in eccentricity to achieve the proper target conditions, the ΔV needed can be calculated simply by

$$\Delta V_{ecc} = 0.5 V_{syn} \sqrt{\Delta e_x^2 + \Delta e_y^2} \tag{7}$$

Finally, the location of the true anomaly for the first maneuver (with all subsequent maneuvers located no less than half a sidereal day apart) can be determined by locating the inertial angle for the change in eccentricity vector. The true anomaly for the maneuver is located parallel to that angle; however, this can have two solutions π radians apart. Care must be taken that the first maneuver be in the vicinity of the initial true anomaly. The true anomaly of the first maneuver can be taken as

$$\nu_0 = \tan^{-1}(\Delta e_y / \Delta e_x) - \alpha_0 \tag{8}$$

where $-90 \leq \tan^{-1}(\Delta e_y / \Delta e_x) \leq 90°$.

If the stationkeeping maneuvers are performed in on-orbit mode, then the ΔV required to control eccentricity and longitude must be divided into a set of smaller ΔV to satisfy the burn duration constraint. The division of the burns is performed in such a fashion as to simultaneously control the longitudinal motion of the spacecraft and set the eccentricity vector to lag the Earth-sun line. Described in the remaining sections of this paper is an algorithm that automatically apportions ΔV_{ecc} into a set of N maneuvers and determines the direction and magnitude of each of these ΔV. Note that all ΔV are assumed to be applied tangentially to the orbit.

IV. Longitude Control Strategy

Before calculating the various ΔV necessary to perform the E/W stationkeeping, a set of initial conditions must be provided to the planning software that is consistent with the maneuver strategy. Table 1 characterizes these boundary conditions. The entries in this table are based on considerations of the geometry associated with changing the eccentricity vector via an impulsive tangential burn combined with the averaged longitudinal acceleration and initial/target longitude and drift rate.

Using this characterization of the boundary conditions, the constraining equations for E/W drift rate and longitude control are developed in the next section. A simplified form of these equations is presented to illustrate a typical maneuver strategy.

A. Eccentricity Targeting Constraint

Based on the control strategy developed earlier, a value for ΔV_{ecc} required to change the eccentricity vector to its target conditions can be determined. By apportioning ΔV_{ecc} to N separate tangential maneuvers, one can write for the four cases in Table 1

$$\Delta V_{ecc} = \begin{cases} \sum_{\substack{i=2 \\ \text{even}}}^{N-1} \Delta V_i - \sum_{\substack{i=1 \\ \text{odd}}}^{N} \Delta V_i, & \text{for case A} \\ \sum_{\substack{i=2 \\ \text{even}}}^{N} \Delta V_i - \sum_{\substack{i=1 \\ \text{odd}}}^{N-1} \Delta V_i, & \text{for case B} \\ \sum_{\substack{i=1 \\ \text{odd}}}^{N-1} \Delta V_i - \sum_{\substack{i=2 \\ \text{even}}}^{N} \Delta V_i, & \text{for case C} \\ \sum_{\substack{i=1 \\ \text{odd}}}^{N} \Delta V_i - \sum_{\substack{i=2 \\ \text{even}}}^{N-1} \Delta V_i, & \text{for case D} \end{cases} \tag{9}$$

where ΔV_i corresponds to the ith maneuver. For convenience Eq. (9) has been formulated assuming that successive ΔV alternate in sign (between orbit-raising and orbit-lowering maneuvers), which may not necessarily be true. In either case, this

Table 1 Boundary conditions

	Initial values[a]				Target values		
Case	True anomaly, ν_0, °	Longitude, λ_0	Drift rate, $\dot{\lambda}_0$	Longitudinal acceleration, $\ddot{\lambda}$	Longitude, λ_T	Drift Rate, $\dot{\lambda}_T$	Number of maneuvers, N
A	≈ 90	−	−	−	−	+	Odd
B	≈ 90	−	−	+	+	−	Even
C	≈ 270	+	+	−	−	+	Even
D	≈ 270	+	+	+	+	−	Odd

[a]Minus sign denotes west and positive sign east.

equation simply constrains the total tangential ΔV (when summed as indicated) to be a positive quantity and equivalent to ΔV_{ecc}.

The velocity increments from a sequence of tangential maneuvers and the resulting change in drift rate, along with Earth-sun-moon effects, are all related by

$$\Delta V_1 = -V_{syn}T_{syn}(\dot{\lambda}_1 - \dot{\lambda}_0)/6\pi$$
$$\Delta V_{i+1} = -V_{syn}T_{syn}(\dot{\lambda}_{i+1} - \dot{\lambda}_i - \ddot{\lambda}_i\Delta t_i)/6\pi \quad (10a)$$

$$(i = 1, 2, \ldots, N-1) \quad (10b)$$

The instantaneous change in drift rate from $\dot{\lambda}_0$, just before the first maneuver, to $\dot{\lambda}_1$, immediately following the first maneuver (hence, $\lambda_0 \equiv \lambda_1$), is related to the initial velocity increment given by Eq. (10a). Similarly, Eq. (10b) relates the subsequent changes in drift rate to the remaining maneuvers and also accounts for the averaged effects of the sun, earth, and moon between maneuvers as

$$\ddot{\lambda}_i \equiv \frac{1}{\Delta t_i}\int_{t_i}^{t_{i+1}} \{\ddot{\lambda}_{tess}[\lambda(t)] + \ddot{\lambda}_{ls}(t)\}\, dt$$
$$\approx \ddot{\lambda}_{tess}(\lambda_s) + \frac{1}{\Delta t_i}\int_{t_i}^{t_{i+1}} \ddot{\lambda}_{ls}(t)\, dt \quad (11)$$

where $\Delta t_i \equiv t_{i+1} - t_i$ referenced to the time of the first maneuver. Note that the change in $\ddot{\lambda}_{tess}$ for excursions in longitude $\mathcal{O}(0.1$ deg) about the station longitude λ_s is negligible. Since the sun, earth, and moon effects are averaged in Eq. (10b), $\dot{\lambda}_i$ is henceforth referred to as the long-period drift rate following the *ith* maneuver.

In the calculation of $\ddot{\lambda}_i$ either a numerical or an analytical method may be used. A numerical average can be obtained by propagating numerically the perturbed satellite orbit (without maneuvers) and forming the discrete average of the longitudinal acceleration over one day (to remove the short periodics) with the average centered on the maneuver time. Double averaging may be necessary to further smooth the results. Alternatively, $\ddot{\lambda}_i$ may be computed by fitting the kinematic equation $\Delta\lambda_i = \dot{\lambda}_i\Delta t_i + \frac{1}{2}\Delta t_i^2\ddot{\lambda}_i$ to the progagated data using $\Delta\lambda_i$ and $\dot{\lambda}_i$ with Δt_i an integral number of days over the free-drift cycle. An analytic average can be obtained utilizing separate expressions for $\ddot{\lambda}_{tess}$ and $\ddot{\lambda}_{ls}$ and then combined according to Eq. (11). For the tesseral harmonics,

$$\ddot{\lambda}_{tess} = 18Q_{22}\sin 2(\lambda_s - \lambda_{22}) - 4.5Q_{31}(\lambda_s - \lambda_{31}) + 135Q_{33}\sin 3(\lambda_s - \lambda_{33}) - 45Q_{42}\sin 2(\lambda_s - \lambda_{42}) + 1260Q_{44}\sin 4(\lambda_s - \lambda_{44}) \quad (12)$$

where

$$Q_{nm} = (R_\oplus/a_{syn})^n\sqrt{S_{nm}^2 + C_{nm}^2},\ (2 < n < 4,\ 0 < m < 4) \quad (13a)$$

$$\lambda_{nm} = (1/m)\tan^{-1}(S_{nm}/C_{nm}) \quad (13b)$$

where S_{nm} and C_{nm} are the spherical harmonics for the Earth's gravity field, and $R_\oplus$ is the Earth's mean equatorial radius. An analytic expression that approximates the satellite's long-period longitudinal acceleration due to the sun and moon can be obtained in a straightforward fashion by twice differentiating with respect to time Eq. (33) given by Kamel and Wagner[4] and then averaging out the short-period terms. It has been demonstrated (using a numerically generated ephemeris) that this analytic ephemeris for longitude contains a secular error (due to missing short-period terms) that results in a longitudinal error of about ±0.005° per 20 days. This in-track error corresponds to approximately a 50-m error in the semimajor axis, which in turn is represented as a bias in the representation of the drift rate. However, the resulting expression for the longitudinal acceleration is not affected by this error.

Equation (10) will be substituted into Eq. (9) and the parameter β defined as

$$\beta \equiv \text{sgn}(-\sin\nu_0) = \begin{cases} +1, & \text{if } \pi < \nu_0 < 2\pi \\ -1, & \text{if } 0 < \nu_0 < \pi \end{cases} \quad (14)$$

A single constraint equation encompassing all four cases can then be written as

$$\dot{\lambda}_0 + 2\sum_{i=1}^{N-1}(-1)^i\dot{\lambda}_i + (-1)^N\dot{\lambda}_N = \frac{6\pi\beta\Delta V_{ecc}}{T_{syn}V_{syn}} - \sum_{i=1}^{N-1}(-1)^i\ddot{\lambda}_i\Delta t_i \quad (15)$$

B. Longitude Displacement Constraint

The desired net long-period displacement in longitude following N maneuvers can be related to the intermediate displacements in longitude as

$$\Delta\lambda_D = \lambda_N - \lambda_0 = \sum_{i=1}^{N-1}(\lambda_{i+1} - \lambda_i) = \sum_{i=1}^{N-1}\Delta\lambda_i \quad (16)$$

This displacement can be expressed in terms of the intermediate drift rates by substituting for $\Delta\lambda_i$ the kinematic equation $\Delta\lambda_i = \dot{\lambda}_i\Delta t_i + \frac{1}{2}\ddot{\lambda}_i\Delta t_i^2$ to give

$$\sum_{i=1}^{N-1}\dot{\lambda}_i\Delta t_i = \Delta\lambda_D - \frac{1}{2}\sum_{i=1}^{N-1}\ddot{\lambda}_i\Delta t_i^2 \quad (17)$$

C. Longitude and Drift Rate Targeting Constraint

Ideally, if the long-period longitudinal acceleration were constant over the free-drift period, the satellite's trajectory in the long-period longitudinal phase plane would be parabolic, centered about the station longitude with its vertex on the λ axis and its drift rate symmetric about this axis. Since the long-period longitudinal acceleration is not constant over the entire

free-drift period, this symmetry cannot be achieved. In any event, expressions for the target longitude and drift rate will be based on the assumption of symmetry by utilizing $\ddot{\lambda}_N$ across the free-drift cycle.

The longitudinal width of the parabolic trajectory is referred to as the soft deadband and is given by

$$\delta\lambda_{sdb} \equiv |\ddot{\lambda}_N|(P_D/2)^2/2 \tag{18}$$

where P_D is the duration of the free-drift period with $\ddot{\lambda}_N$ obtained from Eq. (11) as

$$\ddot{\lambda}_N = \ddot{\lambda}_{tess}(\lambda_s) + \frac{1}{P_D}\int_{t_N}^{t_N + P_D} \ddot{\lambda}_{ls}\, dt \tag{19}$$

This latter expression can be evaluated either numerically or analytically as discussed previously. Hence, the target longitude is given by

$$\lambda_N = \lambda_s \mp \delta\lambda_{sdb}/2 \tag{20}$$

where the minus sign applies to cases A or C, and the plus sign applies to cases B or D. Furthermore, requiring the beginning and ending drift rates on the free-drift cycle to be equal and opposite (i.e., the free-drift cycle begins and ends on the same soft deadband boundary), then from kinematics the drift rate targeting constraint is expressed as

$$\dot{\lambda}_N = -\ddot{\lambda}_N P_D/2 \tag{21}$$

D. Intermediate Drift-Rate Constraints

To affect control of the control cycle size and shape, intermediate drift-rate constraints that contain variable control parameters are introduced. The dimensionless weighting parameter γ_i is defined as

$$\gamma_i = \Delta\lambda_i/\Delta\lambda_D, \qquad (i = 1, 2, \ldots, N-1) \tag{22}$$

which gauges by how much the longitude is walked over in between maneuvers. Summing over the index i and using Eq. (16), one can express the constraint on γ as

$$\sum_{i=1}^{N-1} \gamma_i = 1 \tag{23}$$

Substituting γ_i into the kinematic expressions for $\Delta\lambda_i$ and $\Delta\lambda_{i+1}$ and adding gives the intermediate drift-rate constraints

$$\sum_{k=i}^{i+1} \dot{\lambda}_k \Delta t_k = \Delta\lambda_D \sum_{k=i}^{i+1} \gamma_k - \frac{1}{2}\sum_{k=i}^{i+1} \ddot{\lambda}_k \Delta t_k^2 \qquad (i = 1, 2, \ldots, N-3) \tag{24}$$

Each of these equations helps to constrain the net change in longitude following two successive maneuvers. Note that the limit on the index i may be extended to $N-2$, but only $N-3$ of these constraints can be used to form a deterministic set of equations for the N intermediate drift rates.

The weighting parameters γ_i may be chosen freely subject to the constraint given by Eq. (23). With a view toward shaping the control cycle, these parameters will be defined in terms of the control variables ψ and m by

$$\psi = -\gamma_2/\gamma_1 \quad \text{and} \quad m = \gamma_{i+2}/\gamma_i \qquad (i = 1, 2, \ldots, N-3) \tag{25}$$

Subject to Eq. (23) it can be shown that

$$\gamma_1 = 1/(\sigma_1 - \psi\sigma_2) \tag{26}$$

where

$$\sigma_1 = \sum_{i=0}^{(N-2)/2} m^i \quad \text{and} \quad \sigma_2 = \sum_{i=0}^{(N-3)/2} m^i \tag{27}$$

The parameter ψ is referred to as the longitudinal step factor and influences the size of the longitudinal step per maneuver. It is a ratio of the backward progress in longitudinal translation following the second maneuver to the forward progress following the first maneuver. The second shaping parameter m is interpreted as a magnification factor. Ideally, by decreasing m each successive maneuver will use less ΔV than the previous maneuver, producing a spiraling effect in the longitudinal phase plane. Conversely, as the magnification factor approaches unity, the total ΔV becomes more evenly apportioned among the maneuvers, producing a rectangular box effect. These parameters can be changed to allow flexibility in how ΔV_{ecc} is distributed among the individual maneuvers. Recommended values are

$$0.55 \le m \le 1.0 \quad \text{and} \quad \psi = 0.02 \tag{28}$$

which have been found experimentally (via computer simulation) to produce a generally acceptable long-period longitudinal phase plane trajectory. It should be mentioned that for an odd number of maneuvers and $m = 1.0$ the corresponding constraint equation is insensitive to ψ but is otherwise effective for an even number of maneuvers.

V. Simultaneous Eccentricity and Longitude Control Algorithm

The constraint equations for E/W drift rate and longitude control comprise a system of N linear equations. To facilitate maneuver planning these equations will be simplified by requiring the time between maneuvers to be constant

$$\Delta t_i \mapsto \Delta t = T_{syn}/2, \qquad (\text{for all } i) \tag{29}$$

which corresponds nominally to half a sidereal day. The intermediate maneuver times can then be determined from

$$t_i = t_0 + (i-1)\Delta t, \qquad (i = 1, 2, \ldots, N) \tag{30}$$

where $t_0\,(= t_1)$ is the time of the first maneuver ΔV_1. With this simplification, Eqs. (15), (16), (21), and (24) can be cast in the following matrix form:

$$A\Lambda = \mathbf{B} \tag{31}$$

where

$$A = \begin{bmatrix} -2 & 2 & -2 & 2 & \cdots & 2(-1)^{N-3} & 2(-1)^{N-2} & 2(-1)^{N-1} & (-1)^N \\ 1 & 1 & 1 & 1 & \cdots & 1 & 1 & 1 & 0 \\ 0 & 0 & 0 & 0 & \cdots & 0 & 0 & 0 & 1 \\ 1 & 1 & 0 & 0 & \cdots & 0 & 0 & 0 & 0 \\ 0 & 1 & 1 & 0 & \cdots & 0 & 0 & 0 & 0 \\ 0 & 0 & 1 & 1 & \cdots & 0 & 0 & 0 & 0 \\ \vdots & \vdots & \vdots & \vdots & \ddots & \vdots & \vdots & \vdots & \vdots \\ 0 & 0 & 0 & 0 & \cdots & 1 & 1 & 0 & 0 \end{bmatrix}_{N\times N} \tag{32a}$$

$$\mathbf{\Lambda} = [\dot{\lambda}_1 \ \dot{\lambda}_2 \ \cdots \ \dot{\lambda}_{N-3} \ \ \dot{\lambda}_{N-2} \ \dot{\lambda}_{N-1} \ \ \dot{\lambda}_N]^T \quad (32b)$$

$$\mathbf{B} = [B_{\text{ecc}} \ B_{\Delta\lambda_D} \ B_T \ \ B_1 \ B_2 \cdots B_{N-4} \ \ B_{N-3}]^T \quad (32c)$$

and

$$B_{\text{ecc}} = (6\pi\beta\Delta V_{\text{ecc}}/T_{\text{syn}}V_{\text{syn}}) - \dot{\lambda}_0 - \Delta t \sum_{i=1}^{N-1} (-1)^i \ddot{\lambda}_i \quad (33a)$$

$$B_{\Delta\lambda_D} = (\Delta\lambda_D/\Delta t) - (\Delta t/2) \sum_{i=1}^{N-1} \ddot{\lambda}_i \quad (33b)$$

$$B_T = -\ddot{\lambda}_N P_D/2 \quad (33c)$$

$$B_i = \Delta\lambda_D(\gamma_i + \gamma_{i+1})/\Delta t - \Delta t(\ddot{\lambda}_i + \ddot{\lambda}_{i+1})/2 \quad (i = 1, 2, \ldots, N-3) \quad (33d)$$

with γ_i applicable only for a maneuver scenario that incorporates four or more ΔV.

The intermediate long-period drift rates are obtained by solving Eq. (31) for the drift-rate vector $\mathbf{\Lambda}$ as $\mathbf{\Lambda} = A^{-1}\mathbf{B}$. The N tangential impulsive maneuvers spaced half a sidereal day apart are then obtained from Eq. (10). A positive/negative ΔV corresponds to an orbit-raising/lowering maneuver (i.e., an increase/decrease in orbital energy). Ideally, maneuvers take place near the crossing of the semilatus rectum. In practice, a maneuver is not truly impulsive but rather a series of discrete bursts. This is accounted for by time centering the burst series on the designated time of the maneuver.

Simultaneous control of the mean eccentricity and longitude imposes three constraints on the maneuver strategy: 1) initial conditions, 2) target conditions, and 3) time between maneuvers. Correspondingly, a single maneuver plan exists when this plan is comprised of three maneuvers. Specifically, the maneuver plan is unique in terms of how the ΔV required for eccentricity control is apportioned to the three maneuvers (independent of the burn duration constraint). Furthermore, no maneuver plan (simultaneously satisfying the aforementioned three constraints) exists that consists of two maneuvers since the problem is then overdetermined and an optimal cycle cannot, in general, be achieved. Finally, a maneuver plan that incorporates more than three maneuvers is underdetermined, which introduces a degree of flexibility into how ΔV_{ecc} is apportioned.

VI. Overall Performance

An accurate simulation of the longitudinal motion of a spacecraft in geostationary orbit, embodying the stationkeeping algorithm outlined herein, was performed. This simulation included a model of the orbit determination process to test the robustness of the stationkeeping algorithm to various error sources. These error sources included station location bias, nominal ranging, measurement timing, total thrust vector pointing, thrusting force, thrust command pulse timing, solar radiation pressure force, and the gravity model. A Monte Carlo method of analysis was used. Simulated measurement data was created and fitted using an orbit determination program. A maneuver sequence was computed (based on the determined orbit) and implemented, with the resulting orbit propagated. This process was repeated several times where the end conditions of one stationkeeping cycle became the starting conditions of the next cycle. New noise values were sampled at each stationkeeping cycle for the orbit measurement errors and maneuver execution errors. The maximum and minimum longitude excursions from the station longitude were collected at regular intervals during the entire stationkeeping cycle. Figure 4 is representative of these excursions for both a 7-day and a 14-day stationkeeping cycle. In this figure, data have been superimposed over several concatenated cycles encompassing a total simulation time of 80 weeks.

This figure illustrates the feasibility of the stationkeeping algorithm to maintain longitude control to ± 0.05 deg at or near an equilibrium point in the presence of measurement and execution errors. The number of maneuvers selected by the algorithm is a function of the longitude control size and shaping parameters, annual solar radiation pressure effects, monthly lunar cycle, stationkeeping cycle length, and the initial conditions. For $P_{EW} = 7$ days, the average number of maneuvers was four, and for $P_{EW} = 14$ days the average number of maneuvers was five. As an indication of the algorithm's efficiency, the unused portion of the longitudinal deadband was less than ± 0.005 deg for all stationkeeping cycles.

VII. Concluding Remarks

This paper has developed an algorithm comprised of simple linear algebraic relations that enables the E/W motion of a

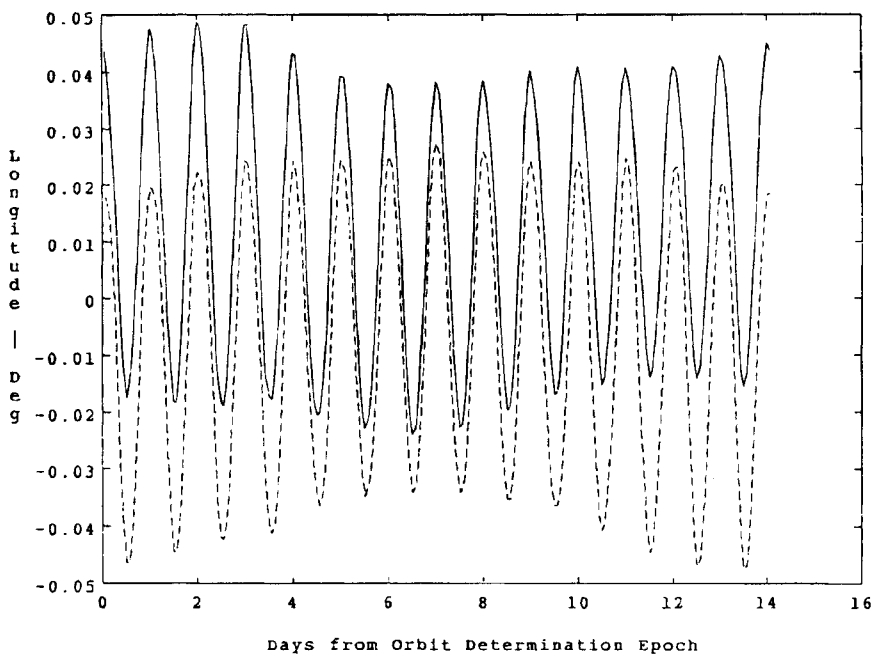

Fig. 4 Eighty-week composite max-min longitudinal excursions (P_{EW} = 14 days and λ_s = 162 deg).

geostationary satellite to be precisely controlled by simultaneously controlling eccentricity and longitude. The stationkeeping maneuvers based on this analysis are by design performed in nominal on-orbit mode, which allows for a reduction in their operational complexity but is equally useful for the stationkeeping mode where large ΔV can be used. The eccentricity control strategy has extended the sun pointing perigee strategy by including the luni-solar effects whereby a more relaxed control of the eccentricity vector length is permitted, resulting in a more efficient use of propellant. The longitudinal control strategy has been expanded to account for the variability in the magnitude and sign of the longitudinal acceleration due to the luni-solar effects. In addition, the maneuvers are apportioned in a novel fashion that allows for the simultaneous control of both eccentricity and longitude. Eccentricity and longitude control variables, whose values were experimentally optimized through simulated operations, have been introduced to provide flexibility in sizing and shaping the maneuver cycle.

This analysis forms the basis of the operational ground-based software used to control the E/W motion of a Japanese communication satellite (SCS-A) built by Ford Aerospace (now Space Systems/Loral) in Palo Alto, California. SCS-A was stationed at longitude 158°E and became operational on July 10, 1989. A second satellite SCS-B identical to SCS-A was to be stationed at longitude 162°E. However, this satellite was lost in the explosion of its launch vehicle in February of 1990. The stationkeeping of both satellites near an unstable equilibrium point coupled with a tight longitudinal deadband requirement (i.e., $\pm 0.05°$) was the primary motivation for considering the long-period luni-solar contribution to the longitudinal acceleration. Also, the large area-to-mass ratio of each satellite motivated the expansion of the SPPS for actively controlling the eccentricity vector. Furthermore, a requirement to perform E/W stationkeeping in on-orbit mode (using the attitude control thrusters), thereby reducing its operational complexity, motivated the apportionment of the total ΔV into N maneuvers.

Areas of current research are directed toward reducing the total number of maneuvers so as to minimize further the operational complexity of the maneuver scenario. For example, by relaxing the target conditions, the minimum number of maneuvers can be reduced to as few as two. For such a maneuver scenario, the satellite would be dropped onto a free-drift cycle that renders the starting and final drift rates not equal and opposite as assumed by Eq. (21). Another method of reducing the number of maneuvers would be to relax the time constraint (i.e., 12h) between maneuvers given by Eq. (29). Through numerical experimentation it has been observed that for some maneuver scenarios the ΔV required for targeting eccentricity is less than the ΔV required to achieve the longitude and/or drift rate target conditions resulting in consecutive maneuvers in the same direction relative to the orbital velocity vector. On occasion this has led to maneuvers that have effectively canceled one another. Methods that would detect such a scenario and collapse the consecutive maneuvers into a single productive maneuver are being investigated.

Acknowledgments

The authors would like to acknowledge the efforts of Ahmed Kamel, Ron Bingaman, and Don Ekman, in particular, as well as many others who contributed to the stationkeeping strategy outlined herein.

References

[1] Kaula, W. M., *Theory of Satellite Geodesy*, Blaisdell Publishing Co., Walthman, MA, 1966.

[2] Lerch, F. J., Klosko, S. M., Patel, G. B., and Wagner, C. A.,"A Gravity Model for Crustal Dynamics (GEM-L2)," *Journal of Geophysical Research*, Vol. 90, No. B11, 1985, pp. 9301–9311.

[3] Lerch, F. J., Klosko, S. M., Wagner, C. A., and Patel, G. B., "On the Accuracy of Recent Goddard Gravity Models," *Journal of Geophysical Research*, Vol. 90, No. B11, 1985, pp. 9312–9334.

[4] Kamel, A. A., and Wagner, C. A., "On the Orbital Eccentricity Control of Synchronous Satellites," *Journal of the Astronautical Sciences*, Vol. 30, No. 1, 1982, pp. 61–73.

[5] Kamel, A. A., Ekman, D. E., and Tibbits, R., "East-West Stationkeeping Requirements of Nearly Synchronous Satellite due to Earth's Triaxiality and Luni-Solar Effects," *Celestial Mechanics*, Vol. 8, 1973, pp. 129–148.

[6] Aksnes, K., "Short-Period and Long-Period Perturbations of a Spherical Satellite Due to Direct Solar Radiation," *Celestial Mechanics*, Vol. 13, 1976, pp. 89–104.

[7] Kamel, A. A., "Geosynchronous Satellite Perturbations Due to Earth's Triaxiality and Luni-Solar Effects," *Journal of Guidance, Control, and Dynamics*, Vol. 5, No. 2, 1982, pp. 189–193.

[8] Eckstein, M. C., "Station Keeping Strategy Test, Design and Optimization by Computer Simulation," *Space Dynamics for Geostationary Satellites*, CEPAD, Toulouse, France, Oct. 1985, pp. 631–677.

[9] Gartrell, C. F., "Simultaneous Eccentricity and Drift Rate Control," *Journal of Guidance, Control, and Dynamics*, Vol. 4, No. 3, 1981, pp. 310–315.

[10] Kechichian, J. A., "A Split ΔV for Drift Rate Control of Geosynchronous Spacecraft," AIAA Paper 83-0017, Jan. 1983.

[11] Gantous, D. J., "Eccentricity Control Strategy for Geosynchronous Communications Satellites," *Telesat Canada*, May 1987.